Increasing the performance of active noise control systems on ground with a finite size vertical reflecting surface

Jiaxin Zhong[1], Jiancheng Tao[1a)], Xiaojun Qiu[2]

[1] Key Laboratory of Modern Acoustics and Institute of Acoustics, Nanjing University, Nanjing, China

[2] Centre for Audio, Acoustics and Vibration, Faculty of Engineering and IT, University of Technology Sydney, Sydney, Australia

a) Author to whom correspondence should be addressed; electric mail: jctao@nju.edu.cn.

Abstract

This paper investigates the feasibility of increasing the noise reduction performance of active noise control systems on ground by introducing a finite size reflecting surface vertical to the ground. By using the image source method and the disk scattering model, the sound radiation power of an active noise control system on ground with an additional finite size semicircular rigid disk vertical to the ground is studied. It is found that the noise reduction of the system can be increased significantly with the infinitely large reflecting surface when the primary and secondary source distance is less than half of the wavelength at the frequency of interest, and the finite size disk can further increase the noise reduction performance at certain bandwidth by up to 2.3 dB. The mechanisms for the performance increase are explored, and the experimental results are presented to validate the analytical and simulation results.

Introduction

In some applications of active sound radiation control, there exist vertical reflecting surfaces, such as the fire barrier walls around the power transformers. These reflecting surfaces and the ground affect the radiation pattern of the sources and the noise reduction performance of Active Noise Control (ANC) systems [1]. However, the effects of finite size reflecting surfaces on ANC systems on ground are rarely studied due to the difficulty of calculating the scattering sound of finite size reflecting surfaces [2].

The ground is typically regarded as an infinitely large rigid plane, and its effects on the noise reduction of ANC systems for sound radiation control have been wildly investigated by using the image source method [3,4]. For single channel ANC systems, the ground reflection can increase the noise reduction if the primary and secondary sources are placed along a line vertical to the ground [5]. The mechanism is that the monopole controlled by one secondary source at low frequency can be approximately considered as a dipole source, and the ground converts a dipole-like source vertical to the ground into a longitudinal quadrupole [6].

For an extended primary source whose characteristic dimensions are comparable to the wavelength, the noise reduction of the ANC system can also be affected by the ground if the geometric center of the source is within 1/5 wavelength from the ground [7]. For multichannel ANC systems, the noise reduction on ground can be maximally increased if the secondary sources are placed as far apart as possible to each other and to the ground [8].

The performance of active control systems near two vertical reflecting surfaces has been studied with numerical simulations [9]. Numerical results show that the noise reduction of the ANC system depends on the elevation angle, the azimuth angle and the distances between the sources and the surfaces. If two reflecting surfaces are optimally placed, more sound reduction of the ANC system can be

achieved compared with that case with only one reflecting surface. The mechanism for the increase of noise reduction is the change of the acoustic impedance caused by the reflecting surfaces. However, the reflecting surfaces considered are infinitely large and there is no experiment validation until now.

A semicircular rigid disk is used in this paper to study the effects of the finite size reflecting surface because the sound field can be analytically solved. A semicircular rigid disk vertically installed on ground can be treated as a rigid disk using the image source method. The scattered sound from this rigid disk can be analytically solved based on the spheroidal wave functions in the oblate spheroidal coordinate system [10]. Although the computation of the spheroidal wave functions is complicated, some software or codes are available online [11–13].

This paper investigates the feasibility of increasing the noise reduction of a single channel ANC system on ground by introducing a vertical reflecting surface. The maximal noise reduction of the ANC system with a finite size semicircular rigid disk vertical to the ground is calculated first by using the analytical disk scattering model, then the effects of the distance between the reflecting surface and the ANC system and the size of the reflecting surface are investigated. The mechanisms for the performance increase are explored, and the experimental results are presented to validate the analytical and simulation results.

Theory

Fig. 1 shows an ANC system on ground with a vertically placed semicircular rigid disk, which has a radius of a and is in the plane $z = 0$. The ground plane is the plane $y = 0$. Therefore, the location of the image source from the ground for a sound source located at (x, y, z) is $(x, -y, z)$. When the source is on the ground plane ($y = 0$), the point source and its image coincides. The distance between the primary and secondary sources is d, and the distance between the secondary source and the center of the disk is l. The semicircular rigid disk vertical to the ground can be

treated as a whole rigid disk using the image source method and its sound radiation can then be calculated based on the disk scattering model [13].

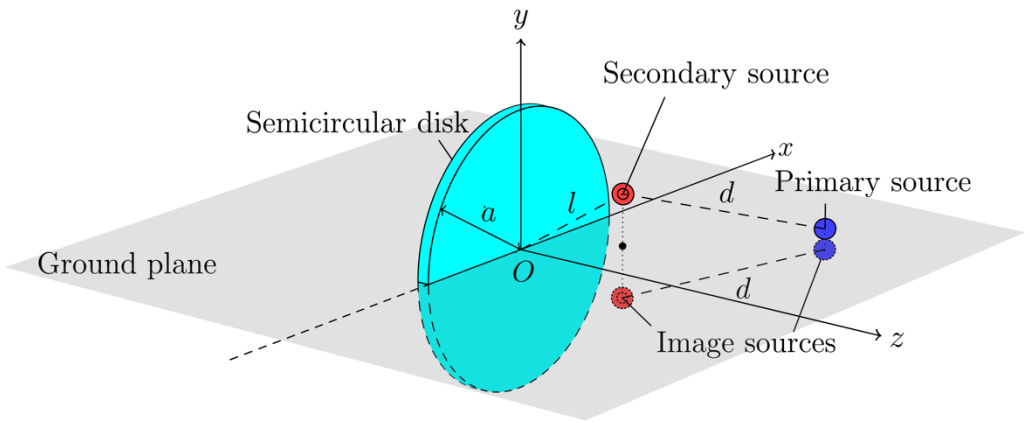

Fig. 1. A single channel ANC system and a semicircular rigid disk with a radius of a on ground where the distance between the primary and secondary sources is d and the distance between the secondary source and the center of the disk is l

The total radiated sound is the superposition of the direct sound from the monopole source and the scattering sound due to the disk. The governing equation of sound field can be solved by using the sound hard boundary condition on the disk surface,

$$\left.\frac{\partial p}{\partial \xi}\right|_{\xi=\xi_b=0} = 0, \tag{1}$$

where ξ is the radial oblate spheroidal coordinate in the oblate spheroidal coordinate system, ξ_b represents the coordinate of the boundary surface, and the oblate coordinates (η, ξ, φ) are related to the Cartesian coordinates (x, y, z) by [10]

$$\begin{aligned} x &= a\sqrt{(1-\eta^2)(1+\xi^2)}\cos\varphi, \\ y &= a\sqrt{(1-\eta^2)(1+\xi^2)}\sin\varphi, \\ z &= a\eta\xi. \end{aligned} \tag{2}$$

When the radial coordinate $\xi = \xi_b = 0$, the oblate represents an infinitely thin disk with a radius of a centered at O on the plane xOy. The oblate coordinates of the

image source of a source above the ground, (η, ξ, φ), is therefore $(\eta, \xi, -\varphi)$. The total sound pressure at a field point (η, ξ, φ) radiated by a monopole source at $(\eta_S, \xi_S, \varphi_S)$ with source strength q is [10]

$$p(\eta,\xi,\varphi)=\frac{\rho_0\omega kq}{4\pi}\sum_{m=0}^{\infty}\sum_{n=m}^{\infty}\frac{2\varepsilon_m}{N_{mn}(-\mathrm{j}ka)}S_{mn}(-\mathrm{j}ka,\eta)S_{mn}(-\mathrm{j}ka,\eta_S)\cos[m(\varphi-\varphi_S)] \times\left[\begin{array}{l} R_{mn}^{(1)}(-\mathrm{j}ka,\mathrm{j}\xi_<)R_{mn}^{(3)}(-\mathrm{j}ka,\mathrm{j}\xi_>) \\ \quad -\dfrac{R_{mn}^{(1)'}(-\mathrm{j}ka,\mathrm{j}\xi_\mathrm{b})}{R_{mn}^{(3)'}(-\mathrm{j}ka,\mathrm{j}\xi_\mathrm{b})}R_{mn}^{(3)}(-\mathrm{j}ka,\mathrm{j}\xi)R_{mn}^{(3)}(-\mathrm{j}ka,\mathrm{j}\xi_S) \end{array}\right], \tag{3}$$

where the harmonic term $\mathrm{e}^{-\mathrm{j}\omega t}$ is omitted, ρ_0 is the air density, ω is the angular frequency of the sound emitted by the source, k is the wavenumber, and ε_m is the Neumann factor i.e. $\varepsilon_m = 1$ for $m = 0$ and $\varepsilon_m = 2$ for $m \neq 0$. The notations follow that in [10], where $S_{mn}(-\mathrm{j}ka, \eta)$ is the angular oblate spheroidal wave function and $N_{mn}(-\mathrm{j}ka)$ is the normalization factor of $S_{mn}(-\mathrm{j}ka, \eta)$, $R_{mn}^{(i)}(-\mathrm{j}ka, \mathrm{j}\xi)$ and $R_{mn}^{(i)'}(-\mathrm{j}ka, \mathrm{j}\xi)$ represent the ith kind of the radial oblate spheroidal wave functions and their derivatives with respect to ξ, $i = 1, 3$, $\xi_< = \min(\xi, \xi_S)$ and $\xi_> = \max(\xi, \xi_S)$.

The mutual radiation resistance between two points $(\eta_i, \xi_i, \varphi_i)$ and $(\eta_j, \xi_j, \varphi_j)$ is

$$Z_{\mathrm{mutual}}\left(\eta_i,\xi_i,\varphi_i;\eta_j,\xi_j,\varphi_j\right)=\frac{\rho_0\omega k}{4\pi}\sum_{m=0}^{\infty}\sum_{n=m}^{\infty}\frac{2\varepsilon_m}{N_{mn}(-\mathrm{j}ka)}S_{mn}(-\mathrm{j}ka,\eta_i)S_{mn}(-\mathrm{j}ka,\eta_j) \times\cos[m(\varphi_i-\varphi_j)]\left[\begin{array}{l} R_{mn}^{(1)}(-\mathrm{j}ka,\mathrm{j}\xi_i)R_{mn}^{(1)}(-\mathrm{j}ka,\mathrm{j}\xi_j) \\ \quad -R_{mn}^{(1)'}(-\mathrm{j}ka,\mathrm{j}\xi_\mathrm{b})\,\mathrm{Re}\left(\dfrac{R_{mn}^{(3)}(-\mathrm{j}ka,\mathrm{j}\xi_i)R_{mn}^{(3)}(-\mathrm{j}ka,\mathrm{j}\xi_j)}{R_{mn}^{(3)'}(-\mathrm{j}ka,\mathrm{j}\xi_\mathrm{b})}\right) \end{array}\right] \tag{4}$$

The self-radiation resistance of a monopole source located at point $(\eta_i, \xi_i, \varphi_i)$ can be obtained by letting $(\eta_i, \xi_i, \varphi_i) = (\eta_j, \xi_j, \varphi_j)$ in Eq. (4) and can be simplified as [13]

$$Z_{\mathrm{self}}\left(\eta_i,\xi_i,\varphi_i\right)=\frac{\rho_0\omega k}{4\pi}\sum_{m=0}^{\infty}\sum_{n=m}^{\infty}\frac{2\varepsilon_m}{N_{mn}(-\mathrm{j}ka)}\left[S_{mn}(-\mathrm{j}ka,\eta_i)\right]^2 \times\left|R_{mn}^{(1)}(-\mathrm{j}ka,\mathrm{j}\xi_i)-\frac{R_{mn}^{(1)'}(-\mathrm{j}ka,\mathrm{j}\xi_\mathrm{b})}{R_{mn}^{(3)'}(-\mathrm{j}ka,\mathrm{j}\xi_\mathrm{b})}R_{mn}^{(3)}(-\mathrm{j}ka,\mathrm{j}\xi_i)\right|^2. \tag{5}$$

The self-radiation resistances of the primary and secondary sources, Z_p and Z_s, and the mutual radiation resistance between these two sources, Z_ps, can be obtained according to Eqs. (4) to (5),

$$Z_{\mathrm{p}} = 2Z_{\mathrm{self}}\left(\eta_{\mathrm{p}}, \xi_{\mathrm{p}}, 0\right), \tag{6}$$

$$Z_{\mathrm{s}} = Z_{\mathrm{self}}\left(\eta_{\mathrm{s}}, \xi_{\mathrm{s}}, \varphi_{\mathrm{s}}\right) + Z_{\mathrm{mutual}}\left(\eta_{\mathrm{s}}, \xi_{\mathrm{s}}, -\varphi_{\mathrm{s}}\right), \tag{7}$$

$$\text{and} \quad Z_{\mathrm{ps}} = 2Z_{\mathrm{mutual}}\left(\eta_{\mathrm{p}}, \xi_{\mathrm{p}}, 0; \eta_{\mathrm{s}}, \xi_{\mathrm{s}}, \varphi_{\mathrm{s}}\right), \tag{8}$$

where $(\eta_{\mathrm{p}}, \xi_{\mathrm{p}}, 0)$ and $(\eta_{\mathrm{s}}, \xi_{\mathrm{s}}, \varphi_{\mathrm{s}})$ are the oblate coordinates of the primary source and the secondary source respectively.

The sound radiation power of a single channel system consisting of one primary source and one secondary source can be formulated as [14]

$$W = A\,|\,q_{\mathrm{s}}\,|^2 + q_{\mathrm{s}}^{*}b + b^{*}q_{\mathrm{s}} + c\,, \tag{9}$$

where $A = 0.5Z_{\mathrm{s}}$, $b = 0.5q_{\mathrm{p}}Z_{\mathrm{ps}}$, $c = 0.5|q_{\mathrm{p}}|^2Z_{\mathrm{p}}$, q_{p} and q_{s} are the complex source strength of the primary source and the secondary source respectively, and the superscript * denotes complex conjugation.

The optimal secondary source strength can be obtained as [14]

$$q_{\mathrm{s,opt}} = -\frac{Z_{\mathrm{ps}}}{Z_{\mathrm{s}}}q_{\mathrm{p}}\,. \tag{10}$$

The minimal sound radiation power under optimal control is then

$$W_{\mathrm{opt}} = \frac{1}{2}\,|\,q_{\mathrm{p}}\,|^2\left(Z_{\mathrm{p}} - \frac{Z_{\mathrm{ps}}^2}{Z_{\mathrm{s}}}\right). \tag{11}$$

The noise reduction is defined as

$$\mathrm{NR} \equiv -10\lg\left(\frac{W_{\mathrm{opt}}}{W_0}\right), \tag{12}$$

where the sound radiation power of the primary source on ground $W_0 = (\rho_0\omega k|q_{\mathrm{p}}|^2)/(4\pi)$ is used as the reference. This defined noise reduction is 0 dB without active noise control if there is no additional reflecting surface around the system. For a constant volume primary source on ground, its sound radiation power (without ANC) varies slightly after introducing a vertical reflecting surface near it. For example, its sound radiation power is increased by 3 dB when an infinitely large reflecting surface is introduced near it at the low frequency. In Eq. (12), the sound

radiation power of the primary source on ground is used as the reference in the definition of the noise reduction, so the NR can then be nonzero (or even negative) without ANC when there is an additional reflecting surface around it.

Substitute Eq. (11) into Eq. (12), the noise reduction can be written in terms of the resistances as

$$\mathrm{NR}=-10\lg\left(\frac{2\pi}{\rho_0\omega k}\frac{Z_\mathrm{p}Z_\mathrm{s}-Z_\mathrm{ps}^2}{Z_\mathrm{s}}\right). \tag{13}$$

It can be found from the equation that the noise reduction increases as the term $(Z_\mathrm{p}Z_\mathrm{s}-Z_\mathrm{ps}^2)/Z_\mathrm{s}$ decreases. According to the reciprocity theorem, the value of $(Z_\mathrm{p}Z_\mathrm{s}-Z_\mathrm{ps}^2)$ does not change if the location of the primary and secondary sources is exchanged, but the value of Z_s might change after the exchanging operation. This implies that higher noise reduction can be obtained if the secondary source is placed in a place where it has higher self-radiation resistance. Therefore, when a reflecting surface is introduced near a single channel ANC system, the surface should be placed close to the secondary source to increase the self-radiation resistance of the secondary source.

Under optimal control the sound radiation power from the secondary source is zero and the total sound radiation power of the system is determined by the self and mutual radiation power of the primary source [8]. Therefore, the primary source should be placed as far as possible to the reflecting surface to make its self-radiation sufficiently small. This implies the line of the primary and secondary sources is vertical to the reflecting surface. It can also be inferred from the vertical dipole mechanism in [6], where it illustrates that the direction of the dipole like source should be placed vertical to the reflecting surface and the primary source should be far away from the rigid surface.

There are different geometry configurations for the primary and secondary sources shown in Fig. 1, which are too many and complicated to be presented in the paper. So, based on the above discussions, this paper only focuses on a specific

configuration where the primary and secondary sources are located on the positive z axis and the disk is placed close to the secondary source. For this special case, the resistances in Eqs. (6) to (8) can be simplified as,

$$Z_{\mathrm{p}} = 2Z_{\mathrm{self}}\left(1, \frac{kd+kl}{ka}, 0\right), \tag{14}$$

$$Z_{\mathrm{s}} = 2Z_{\mathrm{self}}\left(1, \frac{kl}{ka}, 0\right), \tag{15}$$

$$\text{and} \quad Z_{\mathrm{ps}} = 2Z_{\mathrm{mutual}}\left(1, \frac{kd+kl}{ka}, 0; 1, \frac{kl}{ka}, 0\right), \tag{16}$$

where the wavenumber k is not removed in the fractions because the combinations of kl, kd and ka make more sense in the analysis.

A very large disk can be treated as an infinitely large reflecting surface and all the resistances mentioned above can then be directly obtained based on the image source method as,

$$Z_{\mathrm{p}} = \frac{\rho_0 \omega k}{2\pi}\left[1 + \mathrm{sinc}\left(2kd + 2kl\right)\right], \tag{17}$$

$$Z_{\mathrm{s}} = \frac{\rho_0 \omega k}{2\pi}\left[1 + \mathrm{sinc}\left(2kl\right)\right], \tag{18}$$

$$\text{and} \quad Z_{\mathrm{ps}} = \frac{\rho_0 \omega k}{2\pi}\left[\mathrm{sinc}\left(kd\right) + \mathrm{sinc}\left(kd + 2kl\right)\right], \tag{19}$$

where the function $\mathrm{sinc}(x) = \sin(x)/x$.

Simulations and discussions

A MATLAB program was developed to compute the numerical results. The subroutines of spheroidal wave functions were partly referred to the codes provided by Zhang (Chap. 15 in [11]) and was modified for $\xi = 0$ (Section 4.6.2 in [10]). The sound pressure of a monopole source scattering by a rigid disk computed by the MATLAB program has been validated by the boundary element method (BEM) simulation software as described in the authors' paper [13]. In the following simulations, the source distance d is set to 0.1 m and the frequency of interest ranges

from 315 Hz to 5 kHz.

Fig. 2 shows the noise reduction of the ANC system with a vertically placed semicircular disk at a distance l from the secondary source. It is clear that installing the disk closer to the secondary source and using larger disk usually provides better noise reduction performance in the low frequency range. The noise reduction of all cases approaches zero when the frequency is above 1715 Hz, where the source distance d equals the corresponding half wavelength. It should be noted that the noise reduction performance of the system with a vertical reflecting surface can be worse than that without the surface at some frequencies. For example, this frequency range is around 900 Hz when the distance l between the vertically placed semicircular rigid disk and the secondary source is 0.1 m in Fig. 2.

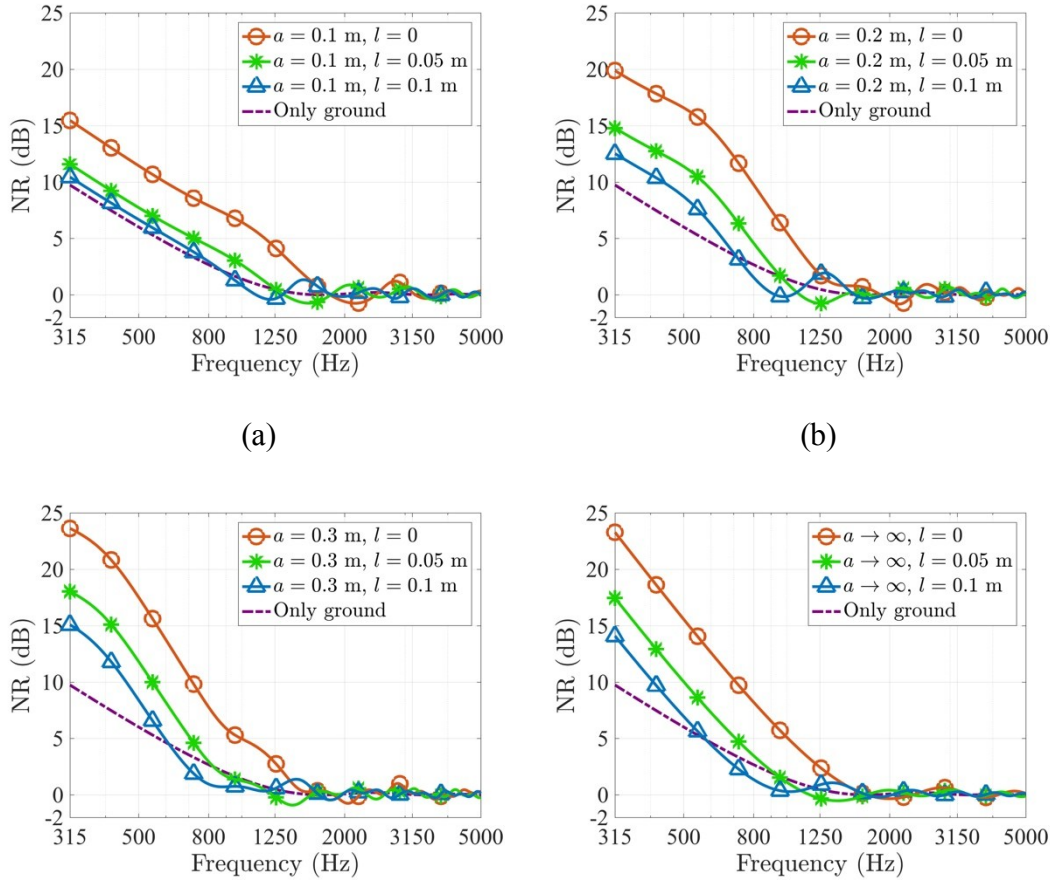

(a) (b)

(c) (d)

Fig. 2. Noise reduction of the ANC system with a vertically placed semicircular

rigid disk at a distance l from the secondary source (a) a = 0.1 m; (b) a = 0.2 m; (c) a = 0.3 m; (d) a is infinitely large

The infinitely large disk case can be employed to illustrate the reason that a smaller distance between the secondary source and the reflecting surface results in large noise reduction. In the very low frequency range, the source strength of the secondary source under optimal control is approximately opposite to that of the primary source, so the primary and secondary sources on ground can be approximately treated as one pair of dipole source with doubled source strength shown in Fig. 3(a). After a vertically placed infinitely large reflecting surface is introduced, the sources are transformed into a longitudinal quadrupole shown in Fig. 3(b), so the noise reduction of the ANC system can be increased because the sound radiation power of a longitudinal quadrupole is usually much less than that of a dipole [6]. A smaller distance between the dipole sources results in smaller the radiation power of the quadrupole.

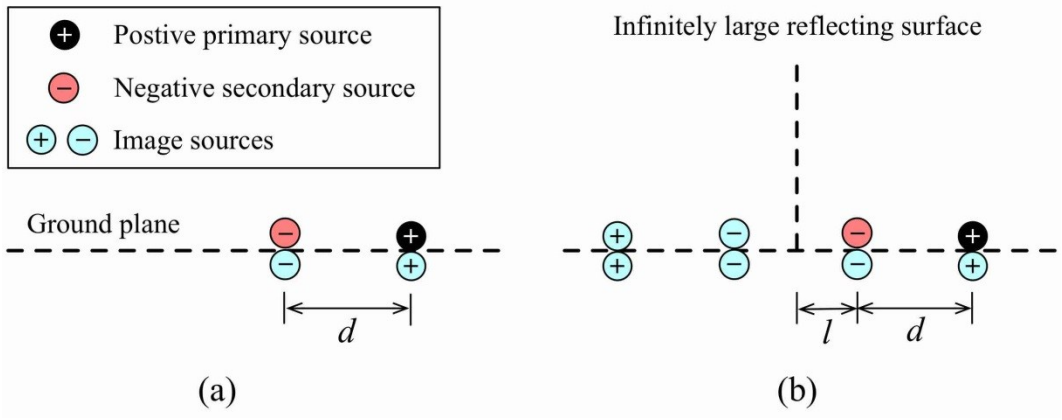

Fig. 3. The equivalent dipole and image sources model at low frequency (a) only the ground (b) a vertically placed infinitely large reflecting surface is presented

For an infinitely large reflecting surface in the low frequency range, the minimal sound radiation power of the ANC system can be expanded from Eqs. (11) and (17) to (19) by using the Taylor series expansion for $k(d + l) < 1$ as

$$W_{\text{opt}} = W_0\left(\frac{2}{45}(kd)^4 + \frac{8}{45}(kd)^3(kl) + \frac{8}{45}(kd)^2(kl)^2 + o\left[(kd)^2\right]o\left[(kl)^2\right]\right), \quad (20)$$

where $o(\cdot)$ represents the order less than the variables inside the parenthesis. Equation (20) indicates that the sound radiation power of the ANC system for a fixed kd increases as the term kl increases and achieves the minimal value when l = 0. Therefore, the reflecting surface should be placed as close as possible to the secondary source for good noise reduction performance and the case l = 0 is the optimal configuration.

To focus on the effects of the disk size, the distance l between the center of the vertically placed semicircular rigid disk and the secondary source is set to 0 in the following simulations. Fig. 4(a) shows that the noise reduction is significantly increased in the low frequency range after introducing the disk. For example, the noise reduction is 6.0 dB at 500 Hz without the disk (i.e. only the ground), and it can be increased up to 17.5 dB by introducing a rigid disk with a radius of 0.3 m.

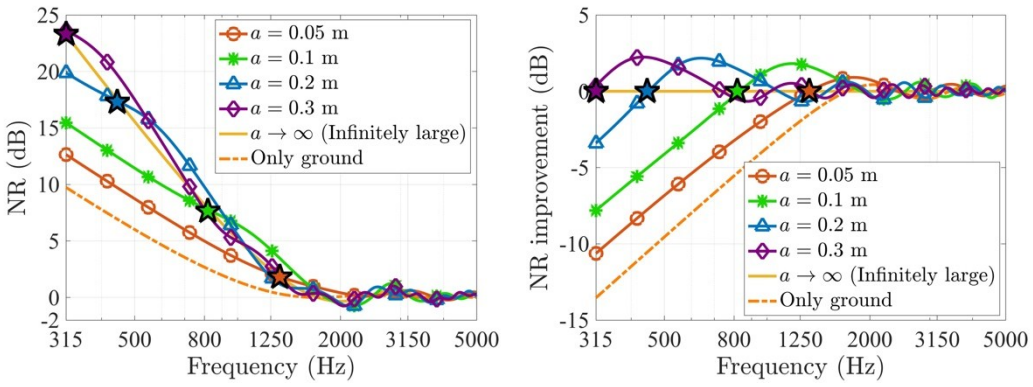

(a) (b)

Fig. 4. The source distance d = 0.1 m (a) Noise reduction of the ANC system for different cases (b) Noise reduction improvement of the ANC system relative to the infinitely large reflecting surface case

The noise reduction improvement of the ANC system relative to the infinitely large reflecting surface is shown in Fig. 4(b). It can be found that the noise

reduction with the infinitely large reflecting surface is usually larger than that with a finite size disk in the low frequency range. In Fig. 4 (a) and (b), the smallest frequency that the noise reduction with the finite size semicircular rigid disk approaches that with the infinitely large one is defined as the cross-frequency, f_c, and is marked is marked by a large solid star maker "★". At some frequencies larger than f_c but less than 1715 Hz, the noise reduction with a finite size disk is larger than that with an infinitely large one. For example, a disk with a radius of 0.3 m brings extra 2.3 dB noise reduction at 440 Hz compared with that with an infinitely large one.

The maxima of the noise reduction improvements in Fig. 4(b) occur at 430 Hz, 640 Hz, and 1180 Hz for the radius a of 0.3 m, 0.2 m, and 0.1 m respectively. These frequencies are around the frequencies corresponding to $a \approx 0.35\lambda$. The sound pressure at the primary source location generated by the secondary source consists of the direct wave and the diffraction wave of the edge of the disk, and the latter one has the maximal constructive effects with the direct wave (even greater than that caused by an infinitely large reflecting surface) when the radius of the disk $a \approx 0.35\lambda$ [13]. Therefore, the sound pressure at the primary source location generated by the secondary source with a disk with a radius of 0.35λ is larger than that with the infinitely large one and the noise reduction of the system is consequently enhanced.

The noise reduction of the ANC system as a function of a/λ and d/λ is shown in Fig. 5, where for a fixed source distance d/λ, the maximal noise reduction of the system is achieved near the line of $a = 0.35\lambda$. Therefore, in practical applications, the distance between the primary and secondary sources can be chosen first according to the practical constraints and then the appropriate radius of the disk can be determined according to the frequency of interest. For example, if the frequency to be controlled is 100 Hz ($\lambda = 3.43$ m) for transformer noise control and the in situ source distance is 0.5 m (0.145λ), the maximal noise reduction of the ANC system

without the reflecting surface is 6.0 dB. With an infinitely large reflecting surface vertically placed on ground, the noise reduction can be increased up to 15.6 dB (using Eqs. (12), (17), (18) and (19)). But if the radius of the semicircular rigid disk is optimized to 1.2 m (0.35λ), the noise reduction can be further increased to 17.7 dB as shown in Fig. 5(a).

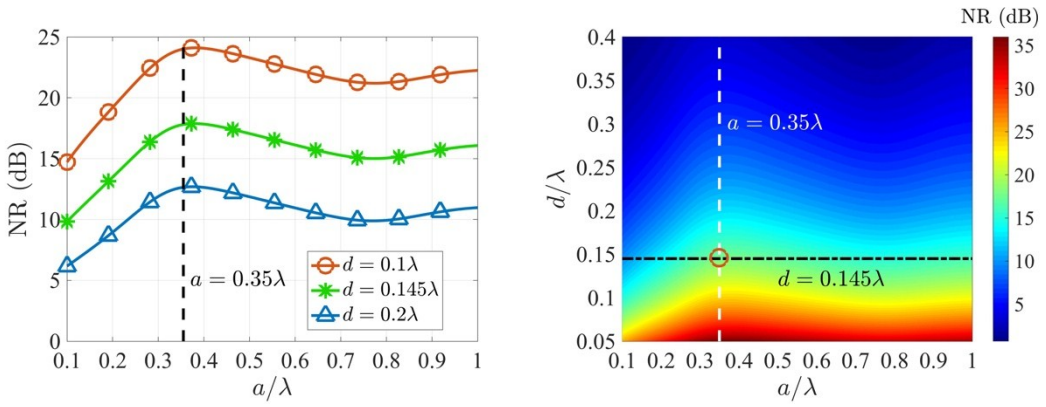

(a) (b)

Fig. 5. (a) Noise reduction of the ANC system as a function of the normalized radius (a/λ) of the semicircular rigid disk at different normalized source distances (b) Noise reduction contour plot of the ANC system as a function of the normalized radius (a/λ) of the semicircular rigid disk and the normalized source distances (d/λ).

Experiments

Experiments with a single channel ANC system were conducted in a full anechoic room in Nanjing University with the dimension of 11.4 m × 7.8 m × 6.7 m as shown in Fig. 6. A wooden plate with an area of 2.4 m × 2.4 m was laid to simulate the infinitely large ground. Two semicircular wooden plates with a radius of 0.1 m and 0.2 m were used as the vertical semicircular rigid disks. In order to facilitate installation, a finite size wooden plate with an area of 1.2 m (height) × 2.4 m was used to simulate the vertical and infinitely large reflecting surface. All the wooden plates used in experiments have a thickness of 1.8 cm and a surface density of 15.30 kg/m^2. According to the Fig. 3 in [15], the effects of the surface density of

wooden plates on sound reflection can be neglected. The ratio of sound power reflected from the wooden plate to the total sound power radiated from the sound source is larger than 96.6% above 100 Hz for a 26.9 m^2 baffle with the surface density of 15.0 kg/m^2 [15].

A semispherical support frame with a radius of 1.5 m was used to install 10 measuring microphones on the top ten positions listed in Table B.2 of ISO 3744 to measure the sound radiation power [16]. The frame is centered at the center of the vertical semicircular disk, which is the midpoint of the line segment intersected by the disk and the ground. The sound pressure at measuring microphones was sampled with a B&K PULSE 3560D system and the FFT analyzer in PULSE LabShop 12.6.1 was used to obtain the FFT spectrum. The frequency span was set to 3.2 kHz with 3200 lines and the averaging type is linear with 66.67% overlap and 30 seconds duration.

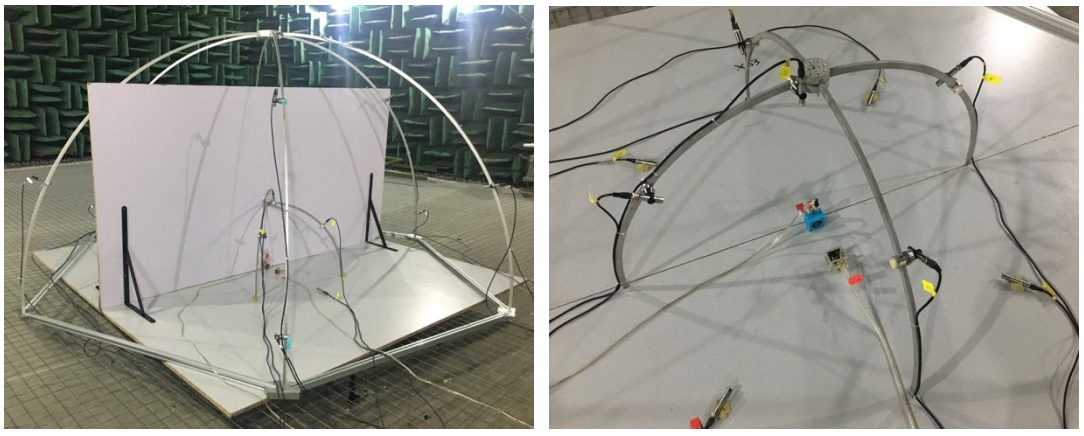

(a) (b)

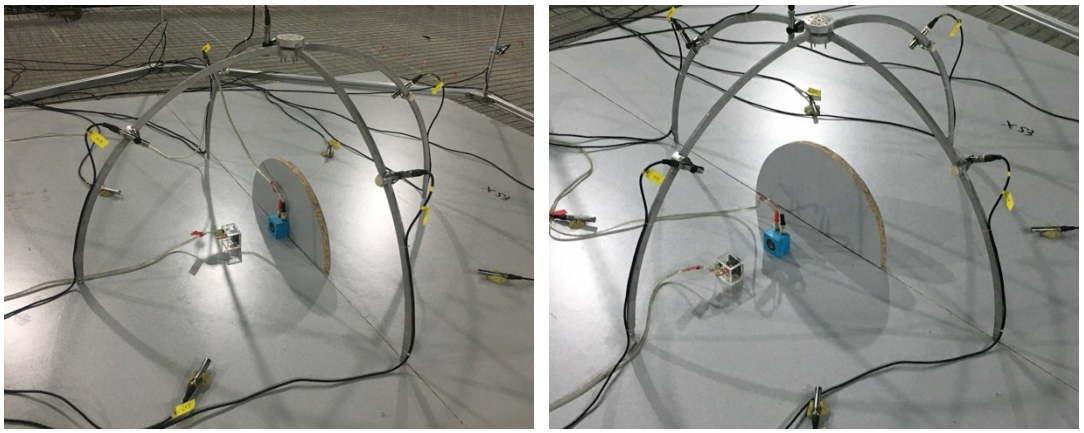

(c) (d)

Fig. 6. Photographs of the experimental setup of a single channel ANC system with a rectangular wooden plate as the ground: (a) a vertically placed and large reflecting surface; (b) only the ground; (c) a vertically placed semicircular rigid disk with a radius of 0.2 m; (d) a vertically placed semicircular rigid disk with a radius of 0.2 m at a distance of 0.1 m to the secondary loudspeaker

A commercial active noise controller (Antysound Tiger ANC WIFI-M) embedded with the waveform synthesis algorithm was used for control [17]. The internally synthesized signal at preset frequencies was used to drive the primary source and adopted as the reference signal. Considering the frequency response of the loudspeakers and the computation capability of the controller, the experiments were conducted at a number of pure tones from 300 Hz to 2 kHz with an interval of 50 Hz.

All the primary and secondary sources are customized loudspeakers, and each source was made by assembling a 1-inch loudspeaker unit in a 48 mm × 48 mm × 38 mm plexiglass box whose sketches are shown in Fig. 7. The sound center of the loudspeaker was considered as the geometric center of the diaphragm of the loudspeaker. Both the two loudspeakers used in experiments were assumed to be omni-directional. The test results by authors (not presented in the paper) show that the maximal deviation of the directional response pattern of the loudspeaker is less than 2 dB below 1 kHz, so the directivity of the loudspeakers does not have significant effects on the experiment results. In the experiments, the minimal distance between the sound center of the secondary source and the vertical disk is 0.038 m when the secondary source was placed close to the vertical disk due to the width of the loudspeaker. The distance between the sound centers of the primary and secondary loudspeakers was set to 0.1 m throughout the experiments.

A semispherical support frame with a radius of 0.5 m centered at the secondary

source was used to install the error microphones as shown in both Fig. 6 and Fig. 7. The ANC process is done by minimizing the sum of the square of the sound pressure at the error microphones. The number and location of error microphones were obtained by simulation before the experiments and the locations for achieving the maximal sound power reduction of the system are given in Table 1 for the case where a vertical semicircular is presented and the case where a large vertical reflecting surface is presented. Further simulations (not presented in this paper) by the authors show that the difference between the sound power reduction by minimizing the sum of the square of sound pressure at these error microphones arrangements and the one by theoretically minimizing the sound power is less than 0.2 dB for the frequency ranges from 300 Hz to 2 kHz.

Table 1 Locations of the error microphones in experiments (1) case I: a vertical semicircular is presented (2) case II: a large vertical reflecting surface is presented

No. of the error mic. i		1	2	3	4	5	6	7	8	9
Case I	Elevation angle θ_i	π/2	π/2	π/4	π/2	3π/4	π/4	π/4	3π/4	3π/4
	Azimuth angle φ_i	π/2	3π/4	π/2	π/4	π/2	π	0	0	π
Case II	Elevation angle θ_i	π/2	π/4	π/4	0	-	-	-	-	-
	Azimuth angle φ_i	π/2	3π/4	π/4	0	-	-	-	-	-

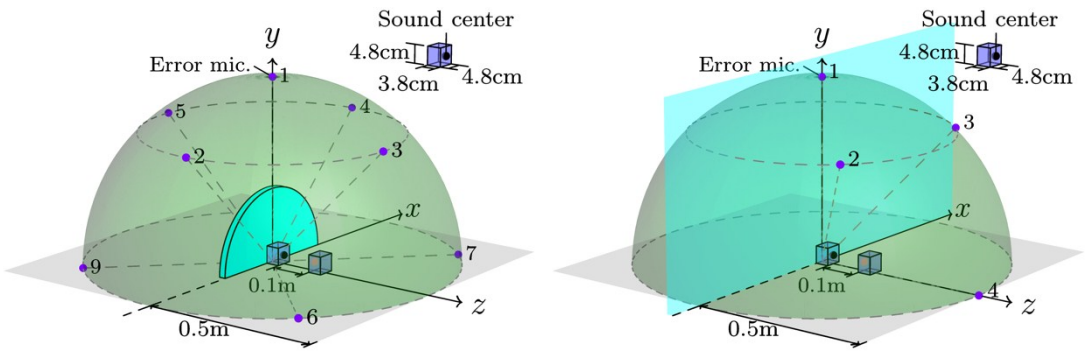

(a) (b)

Fig. 7. Sketch of the locations of the error microphones (a) for the case where a vertical semicircular is presented; (b) for the case where a large vertical reflecting

surface is presented

The measured noise reduction, defined as the measured sound power level with a vertical semicircular disk under optimal control subtracting from the one without the vertical disk and control, is shown in Fig. 8. The radius of the disk is 0.2 m and the distance between the sound center of the secondary source and the vertical disk is set to 0.038, 0.088 m, 0.138 m respectively. It is shown that the variation of experimental results is generally in accordance with the simulation results. The noise reduction becomes larger as the distance between the secondary source and the disk becomes smaller when the frequency is roughly smaller than 850 Hz in this case. Beyond this frequency range, the noise reduction can be larger when the disk is farther from the sources. For example, the noise reduction when $l = 0.038$ m is 3.5 dB in the experiment at 1100 Hz, and it increases to 7.6 dB when $l = 0.138$ m.

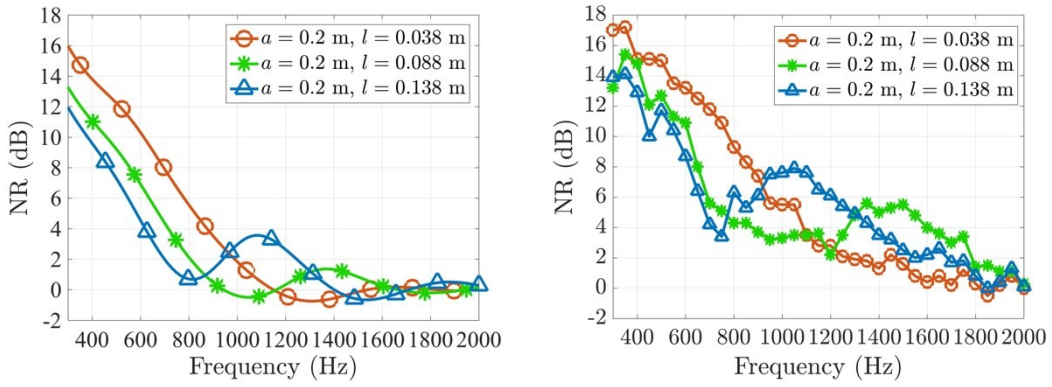

(a) (b)

Fig. 8. Noise reduction with a 0.2 m semicircular disk at different locations (a) simulations; (b) experiments

The measured noise reduction without and with vertical reflecting surfaces is shown in Fig. 9. The variation of experimental results is generally in accordance with the simulation results. Better noise reduction can be achieved at certain frequencies with a finite size and vertical semicircular disk compared to the case

with the large reflecting surface. For example, the noise reduction improvement at 650 Hz by introducing a semicircular disk with a radius of 0.2 m is 3.3 dB higher compared with the case where the large reflecting surface is introduced in the experiment, and the improvement at 1100 Hz by introducing a semicircular disk with a radius of 0.1 m is 2.4 dB higher.

The results in Figs. 8 and 9 show that the noise reductions in the experiments are larger than that in the simulations from 400 Hz to 1600 Hz. This difference may be caused by the following three factors: (1) the measurement uncertainty of the ISO 3744 standard used in the experiments is 3.2 dB with the accuracy grade being "Engineering" level; (2) the locations of sound sources used in the simulations might not be the acoustic center of the loudspeakers in the experiments; and (3) the scattering effects by the loudspeaker boxes. The difference between the experiment and simulation results is not large enough to affect the conclusions drawn in the paper, so no further comprehensive analyses on the difference are presented in the paper.

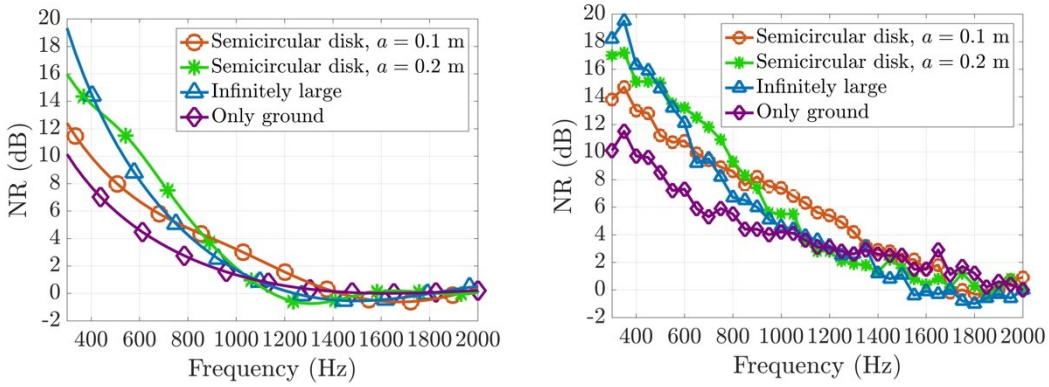

(a) (b)

Fig. 9. Measured noise reduction without and with different vertical reflecting surfaces 0.038 m away from the secondary loudspeaker (a) simulations; (b) experiments

Conclusions

This paper demonstrates that the noise reduction performance of a single channel active noise control system on ground can be significantly increased by introducing a finite size semicircular rigid disk vertical to the ground after optimizing the distance between the secondary source and the disk and the size of the disk. The mechanism for the performance improvement caused by the finite size disk is due to the increased sound pressure diffracted by the edge of the disk at the primary source location generated by the secondary source. To maximize the noise reduction performance of such an ANC system, the vertical reflecting surface should be placed as close as possible to the secondary source and the radius of the disk should be set to 0.35λ where λ is the wavelength of the noise to be controlled. Future research includes exploring the optimal size of a finite size rectangular reflecting surface and applying more reflecting surfaces.

Acknowledgements

This research was supported by the National Science Foundation of China (11474163, 11874218) and under the Australian Research Council's Linkage Projects funding scheme (LP140100740).

References

[1] Qiu X, Lu J, Pan J. A new era for applications of active noise control. Inter-noise 2014, Melbourne, Australia; 2014.

[2] Boodoo S, Paurobally R, Bissessur Y. A review of the effect of reflective surfaces on power output of sound sources and on actively created quiet zones. Acta Acust united Ac 2015;101:877–91.

[3] Ingard U, Lamb GL. Effect of a reflecting plane on the power output of sound sources. J Acoust Soc Am 1957;29:743–4.

[4] Bies DA. Effect of a reflecting plane on an arbitrarily oriented multipole. J

Acoust Soc Am 1960;33(3):286–8.

[5] Cunefare KA, Shepard S. The active control of point acoustic sources in a half-space. J Acoust Soc Am 1993;93(5):2732–9.

[6] Pan J, Qiu X, Paurobally R. Effect of reflecting surfaces on the performance of active noise control. Proceedings of ACOUSTICS 2006, Christchurch, New Zealand; 2006.

[7] Jr. Shepard WS, Cunefare KA. Active control of extended acoustic sources in a half-space. J Acoust Soc Am 1994;96(4):2262–71.

[8] Tao J, Wang S, Qiu X, Pan J. Performance of a multichannel active sound radiation control system near a reflecting surface. Appl Acoust 2017;123:1–8.

[9] Xue J, Tao J, Qiu X. Performance of an active control system near two reflecting surfaces. Proceedings of 20th international congress on sound and vibration, Bangkok, Thailand; 2013.

[10] Flammer C. Spheroidal wave functions. Stanford, CA: Stanford University Press; 1957.

[11] Zhang S, Jin J. Computation of Special Functions. New York: Wiley; 1996. Chap 15.

[12] Adelman R, Gumerov NA, Duraiswami R. Software for computing the spheroidal wave functions using arbitrary precision arithmetic. arXiv 1408.0074 [cs.MS], 2014.

[13] Zhong J, Tao J, Niu F, Qiu X. Effects of a finite size reflecting disk in sound power measurements. Appl Acoust 2018;140:24–9.

[14] Nelson PA, Elliott SJ. Active control of sound. Academic Press; 1992.

[15] Yamada K, Takahashi H, Horiuchi R. Theoretical and experimental investigation of sound power transmitting through reflecting plane with low surface density in the calibration of reference sound sources. Acoust Sci Tech 2015;36(4):374–6.

[16] ISO 3744. Acoustics — Determination of sound power levels and sound

energy levels of noise sources using sound pressure — Engineering methods for an essentially free field over a reflecting plane; 2010.

[17] Qiu X, Hansen CH. An algorithm for active control of transformer noise with on-line cancellation path modelling based on the perturbation method. J Sound Vib 2001;240(4):647–65.